THE JOURNAL OF PHYSICAL CHEMISTRY B

Article

pubs.acs.org/JPCB

Comparative Analysis of Fluorine-Containing Mesogenic Derivatives of Carborane, Bicyclo[2.2.2]octane, Cyclohexane, and Benzene using the Maier−Meier Theory

Piotr Kaszynski,[†,§,*] Adam Januszko,[†,‡] and Kristin L. Glab[†]

[†]Organic Materials Research Group, Department of Chemistry, Vanderbilt University, Nashville, Tennessee 37235, United States

[§]Faculty of Chemistry, University of Łódź, Tamka 12, 91403 Łódź, Poland

Supporting Information

ABSTRACT: Two series of related three-ring nematogens with $\Delta\varepsilon > 0$ and containing 12-vetex carborane (**A**), 10-vertex carborane (**B**), bicyclo[2.2.2]octane (**C**), cyclohexane (**D**) and benzene (**E**) were prepared and investigated as additives to 6-CHBT nematic host and in the pure form (series **2**). Dielectric results were analyzed with the Maier−Meier relationship to gain an understanding of behavior of additives in nematic solutions. Molecular parameters for each nematogen were obtained at the B3LYP/6-31G(d,p) level of theory in the host's dielectric medium, and dielectric data was used as the only experimental parameter to calculate apparent order parameter S_{app} and the Kirkwood factor g. The results demonstrated that compounds in series **1** stabilize the nematic phase (high S_{app}) of the host more than additives in series **2** (low S_{app}), and carbocycles **C** and **D** are more effective (higher S_{app}) than carborane analogues **A** and **B** (lower S_{app}). The method provides insight into behavior of additives in nematic solutions and is useful for comparative analysis of a series of compounds or a series of hosts.

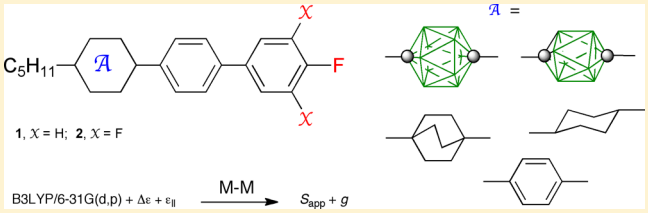

INTRODUCTION

Polar liquid crystals, in which dielectric anisotropy $\Delta\varepsilon$ is controlled by strategic placement of fluorine atoms in the structure,[1] constitute an important class of materials for display applications.[2−9] Such materials are key components of nematic mixtures used, e.g., in thin film transistor liquid crystal display (TFT−LCD) applications,[10] in which high resistivity is essential.[11,12] Evaluation of these materials is typically conducted by extrapolation of bulk parameters, such as $\Delta\varepsilon$, birefringence Δn, and viscosity η, from dilute solutions, e.g., 10 % w/w, in a nematic host. However, electro-optical parameters of the additive, e.g. dielectric permittivity, vary significantly from host to host, due to a different degree of molecular association, dielectric screening, and geometrical compatibility of the additive with the host. For instance, a value $\Delta\varepsilon = 12.0$ was extrapolated for the classical 5CB from a polar host, while $\Delta\varepsilon = 21.8$ was obtained from a weakly polar host.[13]

An important tool used in analysis of nematic compounds[8,13−19] and in designing of new mesogens[6,20−23] for display applications is provided by the Maier−Meier relationship.[24] However, such analyses are conducted typically for pure compounds, thus providing little information about their behavior in nematic mixtures.

The Maier−Meier relationship[24] (eqs 1−3), derived from the Onsager theory for isotropic fluids,[25] connects bulk properties of a liquid crystal, such as dielectric parameters ($\varepsilon_{\parallel}$, $\varepsilon_{\perp}$, and $\Delta\varepsilon$), order parameter S, density (N) and the reaction field and cavity factors (F and h), with their molecular parameters: electronic polarizability (α and $\Delta\alpha$), effective dipole moment (μ_{eff}) and its orientation with respect to the long molecular axes (β).[26−28] The latter parameters can be obtained from quantum-mechanical calculations, and, in conjunction with some experimental data, conveniently provide information on behavior of the material.

$$\Delta\varepsilon = \frac{NFh}{\varepsilon_0}\left\{\Delta\alpha - \frac{F\mu_{eff}^{\ 2}}{2k_BT}(1 - 3\cos^2\beta)\right\}S \quad (1)$$

$$\varepsilon_{\parallel} = 1 + \frac{NFh}{\varepsilon_0}\left\{\bar{\alpha} - \frac{2}{3}\Delta\alpha S + \frac{F\mu_{eff}^{\ 2}}{3k_BT}[1 - (1 - 3\cos^2\beta)S]\right\} \quad (2)$$

$$\varepsilon_{\perp} = 1 + \frac{NFh}{\varepsilon_0}\left\{\bar{\alpha} - \frac{1}{3}\Delta\alpha S + \frac{F\mu_{eff}^{\ 2}}{3k_BT}\left[1 + \frac{1}{2}(1 - 3\cos^2\beta)S\right]\right\} \quad (3)$$

Several years ago we expanded the use of the Maier−Meier relationship to analysis of binary mixtures, which provided information about solvent−solute interactions[29−31] and the degree of aggregation in solution[31] and yielded information about conformer distribution.[32] In this context we investigated

Received: November 18, 2013
Revised: January 30, 2014
Published: February 12, 2014

   dx.doi.org/10.1021/jp411343a | J. Phys. Chem. B 2014, 118, 2238−2248

a series of isostructural compounds containing rings **A**–**E** (Figure 1) with negative dielectric anisotropy ($\Delta\varepsilon < 0$) as

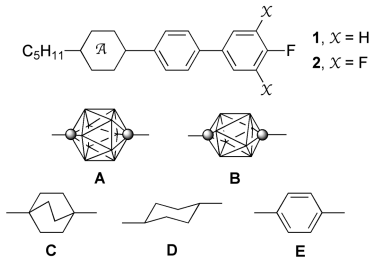

Figure 1. Molecular structures of compounds **1**, **2**, and five ring systems: 1,12-dicarba-*closo*-dodecaborane (12-vertex *p*-carborane, **A**), 1,10-dicarba-*closo*-decaborane (10-vertex *p*-carborane, **B**), bicyclo[2.2.2]octane (**C**), cyclohexane (**D**), and benzene (**E**). In **A** and **B**, each vertex represents a BH fragment and each sphere is a carbon atom.

additives to a nematic host.[29] Analysis of solution dielectric data revealed that the behavior of the additive, most importantly the order parameter *S*, strongly depends on the ring structure in the rigid core. We now focus on a series of three-ring derivatives of fluoro- and 1,2,3-trifluorobenzene with positive dielectric anisotropy ($\Delta\varepsilon > 0$), that belong to a class of materials attractive for TFT–LCD applications.[12,33,34] While analyzing properties of these materials, we refine the protocol for the Maier–Meier analysis.

Here we describe detailed investigation of two series of closely related derivatives **1** and **2** (Figure 1) containing rings **A**–**E** in binary mixtures with a nematic host (6-CHBT) and in the pure form. Experimental dielectric data in conjunctions with theoretical molecular parameters are analyzed using the Maier–Meier formalism providing insight into impact of the ring structure on bulk behavior of these materials. In this context, we (*i*) describe synthetic details and extensive characterization of compounds **1** and **2**, (*ii*) investigate several computational methods for their accuracy in reproduction of molecular electronic parameters, and (*iii*) discuss assumptions used in the Maier–Meier analysis and sources of errors and their impact on analysis results.

EXPERIMENTAL SECTION

General Procedures. Optical microscopy and phase identification was performed using a polarizing microscope equipped with a hot stage. Thermal analysis was obtained using a differential scanning calorimeter (DSC). Transition temperatures (onset) and enthalpies were obtained using small samples (1–2 mg) and a heating rate of 5 K min^{-1} under a flow of nitrogen gas. The clearing transition was typically less than 0.3 °C wide.

Synthetic details and characterization of compounds **1** and **2** are provided in the Supporting Information.

4-(4-*trans*-Hexylcyclohexyl)phenyl isothiocyanate (6-CHBT) was purified by vacuum distillation before use. Dielectric parameters for the pure host were measured 10 times in 3 cells at 25 °C and the results were averaged: $\varepsilon_{\parallel} = 11.79 \pm 0.05$; $\varepsilon_{\perp} = 3.98 \pm 0.03$; $\Delta\varepsilon = 7.80 \pm 0.07$. Literature values:[35] $\varepsilon_{\parallel} = 12.0$; $\varepsilon_{\perp} = 4.0$; $\Delta\varepsilon = 8.0$.

Dielectric Measurements. Properties of compounds in series **1** and **2** were measured with Liquid Crystal Analytical System (LCAS - Series II, LC Analytical Inc.) using GLCAS software version 0.929, which implements literature procedures for dielectric constants.[36]

Approximately 3, 6, and 10 mol % solutions of **1** and **2** in 6-CHBT were prepared and conditioned at 50 °C. The mixtures were loaded into ITO electro-optical cells by capillary action in the isotropic state and measurements were taken at 25 °C. The cells (about 4 μm thick, electrode area of 0.56 cm^2 and antiparallel rubbed polyimide layer) were obtained from LCA Inc. and their precise thicknesses (±0.05 μm) was measured by dielectric methods.

Default parameters were used for measuring dielectric constants of the materials: triangular shaped voltage bias ranging from 0.1 to 15 V at 1 kHz frequency. For each mixture, the measurement was repeated at least 5 times. All consistent results were averaged to calculate the mixture's dielectric parameters. Values for dielectric permittivity $\varepsilon_{\perp}$, $\varepsilon_{\parallel}$, and $\Delta\varepsilon$ were plotted as a function of concentration and using linear regression were extrapolated to pure additives **1** and **2**. The intercept in the fitting functions was fixed at the value for the pure host. The results are presented in Tables 2 and 3. The uncertainties given are the standard errors of the regression's slope at a mole fraction of 1.

Table 1. Transition Temperatures (°C) and Enthalpies (kJ/mol) for Compounds in Series 1 and 2[a]

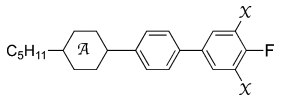

	1 (X = H)	**2** (X = F)
A	Cr 76 N 130 I	Cr 94 (N 72)[b] I[c]
	(22.6) (0.7)	(24.0) (0.2)[d]
B	Cr 104 N 123 I	Cr 46 (N 42)[b] I[c]
	(30.7) (0.5)	(17.6) (0.2)[d]
C	Cr 142 N 197 I[e]	Cr 78 N 105 I[c,f]
	(26.6) (0.6)	(20.5) (0.3)
D	Cr 100 N 152 I[g]	Cr 30 N 56 I[c,h]
	(23.2) (0.7)	(18.9) (0.2)
E	Cr_1 107 Cr_2 210 I	Cr_1 57 Cr_2 94 SmA 97 I[c,i]
	(11.4) (21.2)	(5.1) (7.9) (4.8)

[a]Key: Cr, crystal; Sm, smectic; N, nematic; I, isotropic. Transition temperatures obtained on heating. [b]Monotropic transition. [c]Reference 40. [d]Recorded on cooling. [e]Lit.: Cr 136 N 186 I; ref 44. [f]Lit.: Cr 67 N 78 I; ref 44. [g]Lit.: Cr 100 N 153 I; ref 46. Lit.: Cr 94.3 N 152.8 I; ref 47. [h]Lit.: Cr 30.4 N 58 I; ref 4. Lit.: Cr 29.2 N 57.6 I; ref 34. [i]Lit.: Cr 95.0 Sm 98.5 I; ref 33. Lit.: Cr 94 N 97 I; refs 44 and 45.

A similar method was used for obtaining dielectric data for pure materials. A standard 4 μm electro-optical cell was filled with compound **2** at a temperature slightly above the N–I transition. After 2 h of conditioning, dielectric parameters were measured as a function of temperature to establish the N–I transition ($\Delta\varepsilon \sim 0$) of the material confined to the cell. Attempted measurements for the 12-vertex carborane derivative **2A** were unsuccessful due to sample crystallization upon supercooling by more than 20 K. For compounds **2B**–**2D**, dielectric parameters were measured at several regular temperature intervals from the T_{NI}. Each measurement was repeated at least 5 times and each compound was measured in two different cells. The results were analyzed as described above.

Optical Measurements. Refractive indices n_0 and n_e were measured for homeotropically aligned sample of **2D** using Abbé refractometer at λ = 589 nm at several temperatures. The

dx.doi.org/10.1021/jp411343a | J. Phys. Chem. B 2014, 118, 2238–2248

Table 2. Experimental and Computed Dielectric Parameters for 1[a]

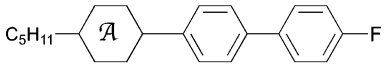

1

	A	B	C	D
Experimental Values for 6-CHBT Solutions, ε_s = 6.60,[b] T = 298 K				
$\varepsilon_\parallel$	7.2 ± 0.1	6.8 ± 0.2	9.1 ± 0.1	9.6 ± 0.1
$\varepsilon_\perp$	2.8 ± 0.05	2.7 ± 0.1	0.9 ± 0.1	1.0 ± 0.1
$\Delta\varepsilon$	4.5 ± 0.1	4.1 ± 0.2	8.2 ± 0.1	8.6 ± 0.1[c]
g[d]	1.10 ± 0.02	0.67 ± 0.04	0.22 ± 0.02	0.36 ± 0.02
S_{app}[d]	0.93 ± 0.02	0.96 ± 0.04	2.71 ± 0.1	2.19 ± 0.07
Computed Values for 6-CHBT Solutions, Assuming ε_s = 6.60,[b] S = 0.67, g = 0.7, T = 298 K				
$\varepsilon_\parallel$	5.4	6.0	7.8	7.6
$\varepsilon_\perp$	3.1	3.1	3.4	3.3
$\Delta\varepsilon$	2.3	2.9	4.4	4.3

[a]For details see text and Supporting Information. [b]Calculated from $\varepsilon_\parallel$ and $\varepsilon_\perp$. [c]Calculated from the components. The extrapolated value has an error of ±0.6. [d]Computed from experimental extrapolated dielectric data using the Maier−Meier relationship and molecular parameters listed in Table 5.

Table 3. Experimental and Computed Dielectric Parameters for 2[a]

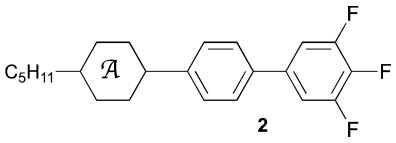

2

	A	B	C	D
Experimental Values for 6-CHBT Solutions, ε_s = 6.60;[b] T = 298 K				
$\varepsilon_\parallel$	10.4 ± 0.1	13.5 ± 0.05	16.5 ± 0.15	13.0 ± 0.15
$\varepsilon_\perp$	4.3 ± 0.2	4.3 ± 0.15	2.9 ± 0.1	3.7 ± 0.1
$\Delta\varepsilon$	6.1 ± 0.1	9.2 ± 0.15	13.6 ± 0.2[c]	9.3 ± 0.2
g[d]	0.69 ± 0.02	0.77 ± 0.02	0.58 ± 0.01	0.51 ± 0.01
S_{app}[d]	0.54 ± 0.02	0.63 ± 0.02	0.93 ± 0.02	0.72 ± 0.02
Computed Values for 6-CHBT Solutions, Assuming ε_s = 6.60,[b] S = 0.67, g = 0.7, T = 298 K				
$\varepsilon_\parallel$	11.5	13.0	16.3	16.0
$\varepsilon_\perp$	3.8	4.0	4.5	4.4
$\Delta\varepsilon$	7.7	9.0	11.8	11.6
Experimental Values for Pure Compound, $T = T_{NI} - 15$ K				
$\varepsilon_\parallel$	e	10.7	10.3	11.6
$\varepsilon_\perp$	e	4.4	4.0	4.5
$\Delta\varepsilon$	e	6.3	6.4	7.1
g	e	0.54	0.46	0.51
S	e	0.54	0.60	0.55

[a]For details see text and Supporting Information. [b]Calculated from $\varepsilon_\parallel$ and $\varepsilon_\perp$. [c]Calculated from the components. The extrapolated value has an error of ±0.4. [d]Computed from experimental extrapolated dielectric data using the Maier−Meier relationship and molecular parameters listed in Table 6. [e]Sample crystallization.

homeotropic alignment was imposed by treating the prisms with lecithin solution in ether.

COMPUTATIONAL DETAILS

Quantum-mechanical calculations were carried out using Gaussian 09 suite of programs.[37] Geometry optimizations for unconstrained conformers of **1** and **2** with most extended molecular shapes were undertaken at the B3LYP/6-31G(d,p) level of theory using default convergence limits. For optimization of test compounds and **2D** additional basis sets and methods were used (including HF and M06). The alkyl groups were in all-*trans* conformation and set *anti* to the C(4)−C(3) bond of the cyclohexane ring in **1D** and **2D**. Final coordinates for each molecular model are provided in the Supporting Information.

Dipole moments and exact electronic polarizabilities of **1** and **2** used in the Maier−Meier data analysis were obtained in 6-CHBT dielectric medium using the B3LYP/6-31G(d,p)//B3LYP/6-31G(d,p) method and the PCM solvation model[38] requested with the SCRF(Solvent=Generic, Read) keyword and "eps=6.60" and "epsinf=2.4623" parameters (single point calculations). The reported values for dipole moment components and dielectric permittivity tensors are at Gaussian standard orientation of each molecule (charge based), which is close to the principal moment of inertia coordinates (mass based). The frequency-dependent calculations were requested with the CPHF keyword.

RESULTS

Materials. Compounds **1** and **2** were prepared by Pd-catalyzed coupling of aryl halide **3** and boronic acids **4** according to a modified Suzuki procedure, using a mixture of *N*-methylpyrrolidone (NMP) and concentrated solution of K_3PO_4 (Scheme 1).[39] This procedure, however, was not

Scheme 1. Synthesis of Compounds 1 and 2

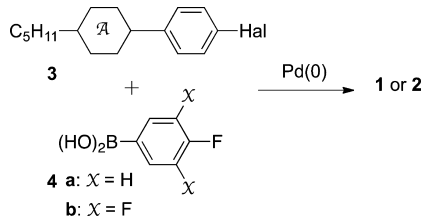

effective for the synthesis of **2B**; only 1-pentyl-10-phenyl-1,10-dicarbadecaborane, product of debromination of starting **3B**, was isolated from the reaction mixture, as evidenced by NMR spectroscopy. The desired compound **2B** was obtained by a different route and its synthesis is described elsewhere.[40]

The preparation of the requisite halides **3A**,[41] **3B**,[42] **3C**,[29] **3D**,[43] and **3E**[29] was reported before.

Thermal Properties. Transition temperatures and enthalpies of the mesogens were determined by differential scanning calorimetry (DSC) and the results are shown in Table 1. Phases were identified by analysis of microscopic textures observed in polarized light.

All terminally fluorinated biphenyls in series **1** and **2** display a nematic phase, while terphenyl derivative **2E** exhibits only a narrow range enantiotropic smectic A phase, as evident from the fan shape texture (Figure 2), and no mesophase was found in **1E** even upon supercooling (Table 1). Our findings for **2E** are consistent with those in another report,[33] however, they are in sharp contrast with literature reports[44,45] of a nematic phase. Also the T_{NI} for **2C** is significantly higher than that previously reported.[44]

The nematic phase stability in series **1** follows the order bicyclo[2.2.2]octane > cyclohexane >12-vertex carborane >10-vertex carborane (**C** > **D** > **A** > **B**), in agreement with findings for other series of isostructural compounds.[29,43,48−52] In series **2**, however, the nematic phase of **2A** is more stable than that

dx.doi.org/10.1021/jp411343a | J. Phys. Chem. B 2014, 118, 2238−2248

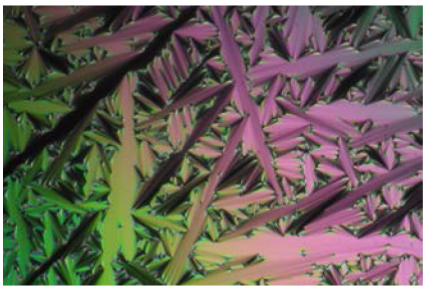

Figure 2. Optical texture of **2E** obtained on cooling from the isotropic phase.

formed by the cyclohexane derivative **2D**, due to less effective shielding against molecular broadening by cyclohexane than the carborane ring.

The depression (ΔT_{NI}) of the clearing temperature T_{NI} in series **1** upon lateral fluorination follows a trend observed before for other series of mesogens.[29,43] The largest destabilization of T_{NI}, by nearly 100 K, is observed for the cyclohexane (**D**) derivative and the smallest for the 12-vertex carborane (**A**) derivative (about 55 K). This is consistent with our previous findings showing that sensitivity of the nematic phase stability to lateral fluorination decreases with increasing ring size and, consequently, more effective shielding of the substituent.[29,43] A plot of ΔT_{NI} versus effective diameter[53] d_e of the variable ring A in the structure is strongly nonlinear (Figure 3). This is in contrast to the results of a similar numerical

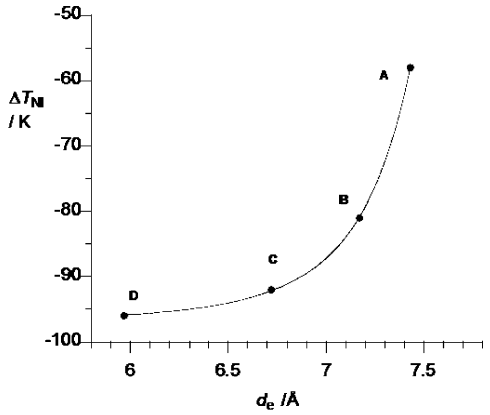

Figure 3. Change in clearing temperatures (ΔT_{NI}) upon fluorination in series **1** plotted as a function of effective VDW diameter d_e of ring A. The line is guide for the eye.

analysis for two other series of mesogens, substituted with an alkyl group at each terminus, for which a linear relationship $\Delta T_{NI}(d_e)$ was found.[29,43]

Optical Measurements. Optical data was collected for the cyclohexane derivative **2D** below the N–I transition and the results are shown in Figure 4. At $T - T_c = -15$ K the nematic phase has a birefringence $\Delta n = 0.151$ and average refractive index $n_{avg} = 1.570$. This compares to $\Delta n = 0.131$ and $n_{avg} = 1.545$ extrapolated from a 10% solution in ZLI-4792.[40] The optical data permitted calculations of the molecular electronic polarizability using the Lorentz–Lorenz relationship (eq 4) and Vuks' model[54,55] (eq 5), $\alpha_{avrg} = 46.8$ Å^3 and $\Delta\alpha = 15.4$ Å^3 at $T - T_c = -15$ K, assuming density of the liquid 1.0 g/cm^3.

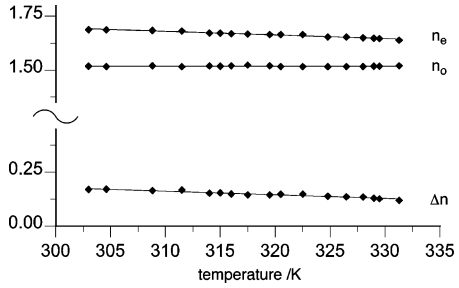

Figure 4. Refractive indices n_e, n_0, and birefringence Δn for **2D** vs temperature.

$$\alpha = \frac{3}{4\pi N}\left\{\frac{n^2 - 1}{n^2 + 2}\right\} \quad (4)$$

$$\Delta\alpha = \frac{3}{4\pi N}\left\{\frac{n_e^2 - n_o^2}{n^2 + 2}\right\} \quad (5)$$

Extrapolation of the optical data to $T = 0$ K from the linear portion of the plot[56] of Δn vs $\log(1 - T/T_c)$ yields the birefringence of ideally ordered material of $\Delta n_{0K} = 0.23 \pm 0.01$. Similar extrapolation of individual optical components n_e and n_0 to $T = 0$ K gave the values $n_{e0K} = 1.748$ and $n_{o0K} = 1.514$, which according to the Vuks' method[54,55] (eq 5) yield $\Delta\alpha_{0K} = 24.0$ Å^3 and $\alpha_{0K} = 48.5$ Å^3 for ideally aligned molecules (order parameter $S_{0K} = 1$). This allows calculation of the order parameter $S = \Delta\alpha / \Delta\alpha_{0K} = 0.64$ at $T - T_c = -15$ K, which is consistent with $S \approx 0.6$ obtained for **2D** from similar optical measurements.[57]

Dielectric Measurements. Compounds in series **1** and **2** were investigated as low concentration additives to a nematic host with positive dielectric anisotropy. The relatively low clearing temperatures in series **2** permitted investigation of dielectric properties of these compounds also in the pure form as a function of temperature. Results for both sets of measurements are collected in Tables 2 and 3. The terphenyl derivatives **1E** and **2E** were not investigated due to their low solubility and lack of a nematic phase.

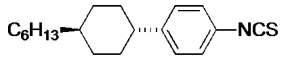

6-CHBT

Solution studies were performed in 6-CHBT ($\Delta\varepsilon = +7.80$) as the host, which was previously used in similar investigations.[29,32,58] For each compound, solutions of typically three concentrations ranging from about 2 mol % to 10 mol % were prepared and their dielectric parameters were measured. Extrapolated values of dielectric constants $\varepsilon_{\parallel}$, $\varepsilon_{\perp}$, and $\Delta\varepsilon$ for compounds **1** and **2** were obtained by linear regression analysis of the solution data to the pure additive. To provide firm bases for comparison of the results, the intercept in the fitting function was set at the appropriate value for the pure host. A sample of data analysis is presented for **1C** in Figure 5, and all results are collected in Tables 2 and 3.[28]

Results for series **1** show that the extrapolated dielectric permittivity values fall in two categories: moderate for the two carborane derivatives **1A** and **1B** and high for the two carbocycles **1C** and **1D**. For the carborane derivatives, the extrapolated $\Delta\varepsilon$ is just above 4, while for **1C** and **1D** the anisotropy is about doubled. These sizable extrapolated $\Delta\varepsilon$ values found for the two carbocycles result from their

dx.doi.org/10.1021/jp411343a | J. Phys. Chem. B 2014, 118, 2238–2248

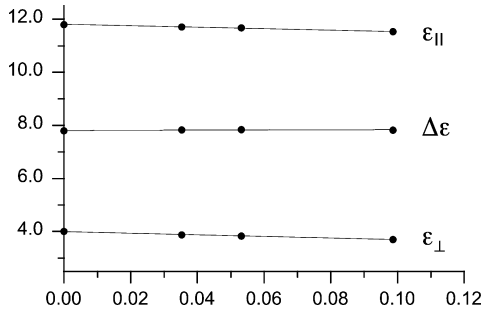

Figure 5. Plot of $\varepsilon_{\parallel}$, $\varepsilon_{\perp}$, and $\Delta\varepsilon$ vs concentration of **1C** in 6-CHBT. Correlation parameters $r^2 > 0.99$ for $\varepsilon_{\parallel}$ and $\varepsilon_{\perp}$.

respectively smaller $\varepsilon_{\perp}$ and larger $\varepsilon_{\parallel}$ in comparison to the carborane derivatives **1A** and **1B**. It is interesting that the extrapolated $\varepsilon_{\perp}$ values for **1C** and **1D** is about 1, which is indicative of increasing order parameter of the solutions (*vide infra*).

Substitution of two additional fluorine atoms to the molecular structure of **1** results in significant increase of all dielectric parameters. A particularly strong effect is observed for the longitudinal components of the dielectric permittivity $\varepsilon_{\parallel}$, which varies between 10.4 for **2A** and 16.5 for **2C**. As a consequence, dielectric anisotropy increases substantially upon fluorination, up to $\Delta\varepsilon = 13.6$ for **2C**. The largest increase in $\Delta\varepsilon$, by about 5, is observed for the 10-vertex carborane (**B**) and bicyclo[2.2.2]octane (**C**), while it is modest for the 12-vertex carborane (**A**, $\Delta\Delta\varepsilon = 1.6$), and surprisingly small, $\Delta\Delta\varepsilon = 0.7$, for the cyclohexane derivatives (**D**). This is presumably related to the reduced molecular anisometry of **2D** upon fluorination of **1D** (see Figure 3), which affects the mixture's order parameter S (*vide infra*) and consequently the value of $\Delta\varepsilon$.

Dielectric parameters extrapolated for **2** from solutions in 6-CHBT (Table 3) are smaller than those obtained from 10% solutions in ZLI-4792 ($\Delta\varepsilon = +5.3$).[40] The biggest difference in extrapolated $\Delta\varepsilon$ values is observed for **2A** ($\Delta\Delta\varepsilon = 2.6$), while only slight increase of $\Delta\varepsilon$ is observed for **2B** ($\Delta\Delta\varepsilon = 0.3$). The differences are mainly due to larger $\varepsilon_{\parallel}$ values in the ZLI host than in 6-CHBT.

Dielectric properties of three pure compounds in series **2** were measured at several shifted temperatures and results for $T = T_{NI} - 15$ are shown in Table 3. The neat 12-vertex carborane derivative **2A** could not be measured due to rapid crystallization of the supercooled material in a measuring cell. Results show that all three compounds, **2B**, **2C**, and **2D** have comparable dielectric paramaters with $\Delta\varepsilon$ in a range of 6.3 (**2B**) to 7.1 (**2D**). These values are significantly lower than those extrapolated from solutions in 6-CHBT (Table 3) or in ZLI-4792.[40]

Computation of Molecular Parameters. For rationalization of the experimental dielectric data the necessary dipole moments μ and electronic polarizabilities α could be obtained from quantum-mechanical calculations.[59] Since the calculated values are method-depended, several computational methods were screened using PhF, PhCN, *m*-$C_6H_4F_2$, and 5CB as model compounds.[28] Results demonstrated that DFT methods (B3LYP and M06) give higher values for α and lower for μ than the HF method with the same basis set in vacuum. Larger basis sets increase both values, but polarizability is still short of the experimental values. Results close to the experimental values of α were obtained with standard basis set augmented with diffuse functions or by using the polarizable continuum (PCM) solvation model.[38] The latter method overestimates the dipole moment for PhCN; however, the measured dipole moment values depend on the experimental method and medium.[60,61] Fortunately, any systematic errors in treatment of **1** and **2** are included in the empirical Kirkwood factor g,[62] and comparison of results for the same medium and computational method should be self-consistent. Results for **2D** obtained with several computational methods are shown in Table 4.

Data in Table 4 shows that DFT methods augmented with diffuse functions or in conjunction with the PCM solvation model perform well and the electronic polarizability α_{avrg} calculated for **2D** is close to the experimental value of about 46 Å^3 obtained form optical measurements at 589 nm. However, the calculated polarizability anisotropies $\Delta\alpha$ are uniformly high and about 30 Å^3, which is higher approximately by about 25% than the experimental values. Even higher anisotropy is calculated at 589 nm ($\Delta\alpha = 35.5$ Å^3). Such a discrepancy between measured and calculated values has been noticed by others.[21] The calculated molecular dipole moment values are generally about 4.4 D, while the smallest value of 3.8 D was calculated with the 6-31G(d,p) basis set in vacuum. The variation in the calculated values of polarizability and dipole moment has rather small effect on the order parameter S.

Table 4. Calculated Molecular and Phase Parameters for 2D at $T - T_{NI} = -15$ K and 6-CHBT Solutions

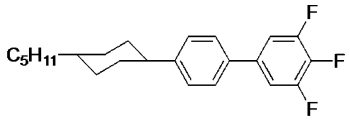

							neat[c]		6-CHBT[d]	
parameter method	$\mu_{\parallel}$/D	$\mu_{\perp}$/D	μ/D	β^a/deg	$\alpha_{avrg}{}^b$/Å^3	$\Delta\alpha^b$/Å^3	g	S	g	S_{app}
HF/6-31G(d,p)	4.43	0.57	4.47	7.4	34.0	24.0	0.65	0.49	0.52	0.69
B3LYP/3-21G	4.17	0.61	4.21	8.3	34.9	29.0	0.71	0.50	0.58	0.66
B3LYP/6-31G(d,p)	3.77	0.49	3.80	7.3	37.7	30.6	0.80	0.50	0.69	0.67
B3LYP/6-31G(d,p) and PCM[e]	4.24	0.56	4.28	7.6	45.3	30.0	(0.51)	(0.55)	0.51	0.72
					44.3[f]	35.5[f]				
B3LYP/6-31++G(2d,p)// B3LYP/6-31G(d,p)	4.43	0.55	4.46	7.1	42.7	31.2	0.51	0.53	0.48	0.70
experimental	–	–	–	–	48.5[g,h]	24.0[g,h]	–	0.64[h]	–	0.76[h]
					45.1[i]	–				

[a]Angle between the net dipole vector μ and long molecular axes calculated from the vector components. [b]Static field. [c]At $T - T_{NI} = -15$ K. [d]6-CHBT solutions. [e]6-CHBT dielectric medium. [f]Calculated at 589 nm. [g]Optical values at $T = 0$ K. [h]This work. [i]From data reported in ref 40.

dx.doi.org/10.1021/jp411343a | J. Phys. Chem. B 2014, 118, 2238−2248

Nevertheless, considering accuracy and efficiency of the calculations, the B3LYP/6-31G(d,p) method with the PCM solvation model was chosen for obtaining molecular parameters of compounds in series **1** and **2** for analysis of the dielectric data.[28]

Table 5. Calculated Molecular Parameters for 1[a]

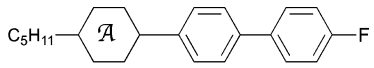

1

	A	B	C	D	E
$\mu_{\parallel}$/D	1.59	1.76	2.40	2.26	2.26
$\mu_{\perp}$/D	0.09	0.01	0.27	0.26	0.13
μ/D	1.59	1.76	2.41	2.28	2.27
β[b]/deg	3	0	6	7	3
$\Delta\alpha$[c]/Å^3	37.6	39.6	32.6	30.1[d]	45.4
α_{avrg}[c]/Å^3	58.0	54.9	50.6	45.1	47.8

[a]Obtained with the B3LYP/6-31G(d,p) method in 6-CHBT dielectric medium. [b]Angle between the net dipole vector μ and long molecular axes calculated from the vector components. For details see the Supporting Information. [c]Static field. [d]$\Delta\alpha$ = 19.5 Å^3 calculated from anisotropy of bond polarizability in arbitrary coordinates; ref 47.

Results in Tables 5 and 6 show that the transverse dipole moment $\mu_{\perp}$ is small (<0.6 D) for all derivatives **1** and **2**. In contrast, the longitudinal dipole moment component $\mu_{\parallel}$ is significant and in a range of 1.6−2.4 D in series **1** and higher by about 2 D in series **2**. Consequently, the net molecular dipole moment vector is nearly parallel to the long molecular axis ($\beta \leq 7°$). The value of $\mu_{\parallel}$ varies in both series of compounds, which reflects the electron withdrawing ability of the ring A and correlates well with the ring σ_p parameter:[63] **A** (σ_p = 0.12)[64] **B** (σ_p = 0.04)[65] **C** (σ_p = −0.13),[66] **D** (σ_p = −0.15),[67] and **E** (4-EtPh, σ_p = −0.02).[67] As expected, the observed trend in the $\mu_{\parallel}$ is largely consistent with the trend in the extrapolated values of $\varepsilon_{\parallel}$.

The calculated average static electronic polarizability α_{avrg} decreases in both series from about 58 Å^3 for derivatives of the most polarizable 12-vertex carborane **A** to about 45 Å^3 for the cyclohexane derivatives (**A** > **B** > **C** > **E** > **D**). Anisotropy of electronic polarizability $\Delta\alpha$ follows a different trend and is largest for the terphenyl derivatives **E**, about 45 Å^3, and smallest for the aliphatic rings. The overall trend in $\Delta\alpha$ (**E** > **B** > **A** > **C** > **D**) reflects the differences between the types of electronic structures: highly delocalized *vs* localized (aliphatic), and shapes of the rings. Thus, the highest anisotropy is observed for the compounds containing the π-aromatic (**E**) or σ-aromatic (**A** and **B**) rings. However, the 3-dimensional distribution of electrons in carboranes **A** and **B** gives rise to smaller anisotropy $\Delta\alpha$ than that observed for the benzene derivatives **E**.[68] These observed trends in α_{avrg} and $\Delta\alpha$ are consistent with the order of refractive indices extrapolated from ZLI-4792 solutions for **2A**, **2B**, and **2D**,[40] and also with our findings for another series of mesogens.[58]

A comparison of theoretical with experimental electronic polarizabilities demonstrates that the calculated values of α_{avrg} (Table 6) are close to those obtained from optical measurements for pure **2D** and also for **2A**, **2B** and **2D** in ZLI-4792 solutions.[40] It appears, however, that the calculated $\Delta\alpha$ values are significantly larger than those established experimentally, e.g. calculated $\Delta\alpha_{theory}$ = 30.1 Å^3, while $\Delta\alpha_{exptl}$ = 24.0 Å^3 for ideally aligned molecules of **2D** (S = 1, *vide supra*). Similarly, assuming a conservative order parameter S = 0.67 for solutions of **2A**, **2B** and **2D** in ZLI-4792,[40] $\Delta\alpha_{exptl}$ values are also significantly smaller that those calculated with the DFT method at static field.

Dielectric Data Analysis. Results of dielectric measurements for binary mixtures and pure compounds were analyzed quantitatively using the Maier−Meier relationship (eqs 1−3). Molecular parameters α, μ, and β were obtained computationally and are listed in Tables 5 and 6. The reaction field F and cavity factor h for pure compounds **2** were obtained from experimental dielectric data and calculated polarizability, while dielectric parameters $\varepsilon_{\parallel}$, $\varepsilon_{\perp}$ and $\Delta\varepsilon$ were obtained by direct experiment. The density of the liquids was assumed to be 1.0 g/cm^3. The remaining two quantities in eq 1, the order parameter S and the Kirkwood factor[62] g, are the only adjustable parameters in the equation. Both of them were calculated using eqs 6 and 7 obtained by solving simultaneously expressions for $\varepsilon_{\parallel}$ (eq 2) and $\Delta\varepsilon$ (eq 1). The results are shown in Tables 2 and 3. For calculations involving binary mixtures, the medium was assumed to be that of the pure host, and the effect of the additive was neglected. Therefore, factors F and h for 6-CHBT were obtained from experimental optical[69] and dielectric data using the Dunmur-Toriyama relationship.[26] Further details are provided in the Supporting Information.

Table 6. Calculated Molecular Parameters for 2[a]

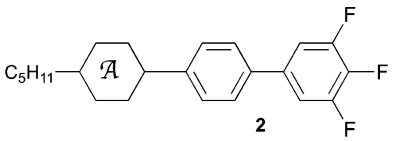

2

	A	B	C	D	E
$\mu_{\parallel}$/D	3.64	3.82	4.42	4.24	4.35
$\mu_{\perp}$/D	0.07	0.15	0.45	0.56	0.35
μ/D	3.64	3.82	4.44	4.28	4.37
β[b]/deg	0	2	6	7	4
$\Delta\alpha$[c]/Å^3	37.0 (19.9)[d]	39.3 (21.5)[d]	32.6	30.1[e] (19.9)[d]	45.5
α_{avrg}[c]/Å^3	58.0 (55.2)[d]	55.0 (51.6)[d]	50.8	45.3[e] (45.1)[d]	48.0

[a]Obtained with the B3LYP/6-31G(d,p) method in the 6-CHBT dielectric medium. [b]Angle between the net dipole vector μ and long molecular axes calculated from the vector components. For details see Supporting Information. [c]Static field. [d]From optical data extrapolated from ZLI-4792 solutions and assuming order parameter S = 0.67; ref 40. [e]Experimental α_{avrg} = 48.5 Å^3 and $\Delta\alpha$ = 24.0 Å^3 at T = 0 K (this work).

dx.doi.org/10.1021/jp411343a | J. Phys. Chem. B 2014, 118, 2238−2248

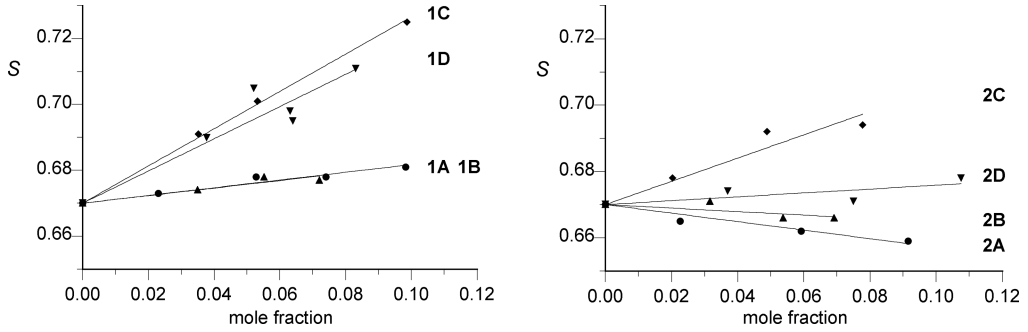

Figure 6. Plot of the order parameter S for 6-CHBT solutions vs mole fraction of **1A**−**1D** and **2A**−**2D**. Parameter S was calculated using eq 10. Details are in the text and the Supporting Information.

$$S = \frac{2\Delta\varepsilon\varepsilon_0}{NFh[2\Delta\alpha + 3\bar{\alpha}(1 - 3\cos^2\beta)] - 3(\bar{\varepsilon} - 1)\varepsilon_0(1 - 3\cos^2\beta)} \quad (6)$$

$$g = \frac{\left[(\varepsilon_{\parallel} - 1)\varepsilon_0 - \bar{\alpha}NFh - \frac{2}{3}\Delta\alpha NFhS\right]3k_BT}{NF^2h\mu^2[1 - (1 - 3\cos^2\beta)S]} \quad (7)$$

Initially, dielectric parameters for compounds **1** and **2** in ideal 6-CHBT solutions were calculated using the Maier−Meier relationship with the assumption that their order parameter is the same as for the pure host (S_{host} = 0.67 at 25 °C),[14] and about 14% of the theoretical dipole moment is compensated (g = 0.7). Results collected in Tables 2 and 3 show, not surprisingly, that the trends in $\varepsilon_{\parallel}$ and $\Delta\varepsilon$ generally parallel those for the computed $\mu_{\parallel}$ and μ and the highest values in each series were found for the terphenyl derivatives (**1E**, $\varepsilon_{\parallel}$ = 8.1 and $\Delta\varepsilon$ = 4.9; **2E**, $\varepsilon_{\parallel}$ = 17.3 and $\Delta\varepsilon$ = 12.9). The transverse component $\varepsilon_{\perp}$ is approximately 3.5 for **1** and about 4.5 for **2**. A comparison of these values predicted for ideal solutions in 6-CHBT with those extrapolated form experimental data shows some significant differences.

Experimental dielectric parameters for carborane derivatives **1A** and **1B** are generally within 1 unit of the values predicted for ideal solutions, while significant discrepancies are found for dielectric parameters of carbocycles **1C** and **1D**. Their extrapolated $\varepsilon_{\perp}$ values are lower by about 2, and, consequently, dielectric anisotropy $\Delta\varepsilon$ values are markedly higher than predicted. Similar, albeit smaller differences were found in series **2**.

More insight into solute−solvent interactions is offered by analysis of the apparent order parameter[29] S_{app} and g values in both series (Tables 2 and 3) obtained from the extrapolated dielectric data. The S_{app} can be viewed as an "activity parameter" for the additive in the expression for mixture's dielectric anisotropy (eqs 8 and 9). In general, order parameter S_{app} is related to the T_{NI} of the additive and geometrical compatibility with the host, while the Kirkwood factor g reflects the effective molecular polarity in condensed phase. Thus, it can be expected that the higher T_{NI}, the higher S_{app}, and also the larger μ the smaller g. Indeed, in series **1** of weakly polar additives the S_{app} and T_{NI} exhibit a similar trend **1C** > **1D** > **1A** ∼ **1B**. All values S_{app} are higher than the order parameter for the host (S_{host} = 0.67 at 25 °C),[14] which indicates that all four additives increase the S value of the solution and stabilize the nematic phase. Also, as expected, the Kirkwood factor g follows the trend **1A** > **1B** > **1C** ∼ **1D**, which is a reverse of the trend in values of molecular dipole moment in the series.

In the series of more polar derivatives **2**, the trends are less clear. The S_{app} values follow the order **2C** > **2D** > **2B** > **2A**, which, with the exception of **2A**, follows the trend in T_{NI} of the compounds. Among the four additives, only **2C** and **2D** stabilize the nematic phase (S_{app} = 0.93 and 0.72, respectively), while for the two carborane derivatives, **2A** and **2B**, S_{app} < 0.67 (Table 3). Values for the Kirkwood factor g in series **2** fall into a range of 0.51 (**2D**) and 0.77 (**2B**), which is typical for moderately polar nematic compounds.[14,70] Similar results were obtained from analysis of dielectric data for pure compounds in series **2** (Table 3) and the calculated values for S and g fall into the expected ranges: 0.54−0.60 for S, and 0.46−0.54 for g.

$$\Delta\varepsilon = \Delta\varepsilon_{add}x + \Delta\varepsilon_{host}(1 - x) \quad (8)$$

$$\Delta\varepsilon = C_{add}S_{app}x + C_{host}S_{host}(1 - x) \quad (9)$$

$$\Delta\varepsilon = S[C_{add}x + C_{host}(1 - x)] \quad (10)$$

The dielectric permittivity data can be analyzed in another way with the focus on the overall order parameter of a binary mixture. Since the Maier−Meier relationship (eq 1) can be presented as a product of the molecular parameter C ($\Delta\varepsilon$ for ideally ordered material) and order parameter S, the expression for $\Delta\varepsilon$ of the binary mixture (eq 8) can be written as eq 9, in which x represents mole fraction, C_{add} and C_{host} are the molecular parameters and S_{app} and S_{host} are individual order parameters of the additive and the host, respectively. It is reasonable to assume that all components of the mixture have the same order parameter, which leads to eq 10. With this equation, the common order parameter S can be calculated for each mole fraction x of the additive in the binary mixture using individual molecular parameters, C_{add} and C_{host}, and the experimental $\Delta\varepsilon$. Results are shown in Figure 6 and numerical data are given in the Supporting Information.

Analysis of the plots shows that compounds in series **1** increase the mixture's order parameter (stabilize the nematic phase) more than compounds in series **2**, and that the effectiveness in increasing the mixture's order parameter S follows the order **A** < **B** < **D** < **C**. These results are consistent with the analysis of apparent order parameter S_{app}, and demonstrate once again the lowest compatibility of the voluminous carborane cages with the nematic host. A similar trend in the impact of the rigid core structure on phase behavior and dielectric properties was found for another series of compounds containing the four ring systems **A**−**D**.[29]

dx.doi.org/10.1021/jp411343a | J. Phys. Chem. B 2014, 118, 2238−2248

DISCUSSION

The implementation of the Maier−Meier theory in this work relies on experimental data for the host (dielectric data, refractive index, and density) to derive reaction field and cavity parameters F and h, experimental dielectric data for solutions, and calculated molecular properties of the additive: dipole moment components and polarizability tensors. The latter, more precisely anisotropy of polarizability, contains the only information about the additive's anisometry used in the theory. The assumed cylindrical shape of the molecule and the isotropic reaction field are two of several approximations in the Maier−Meier formalism.

Molecular parameters α and μ are typically calculated using either quantum-mechanical methods or group increments. The calculations are usually performed in vacuum rather than in condensed phase and the accuracy of the calculations depends on the level of theory and the presence of heaver elements. The issue of precision of such calculations is additionally complicated by the medium- and measurement method-dependence of the experimental values, especially for the dipole moments.[60,61] Lower uncertainty is associated with experimental values of electronic polarizability α, although direct comparison with theoretical data is complicated by often unknown density of the nematic phase and dispersion of the optical data.[71] Nevertheless, closest agreement between experiment and theory was observed for values α calculated with inclusion of dielectric medium of the condensed phase. Interestingly, polarizability anisotropy $\Delta\alpha$ is overestimated with essentially all higher-level computational methods tested here, which ultimately has impact on phase parameters g and S_{app}. For example, for **2D** order parameter S_{app} is larger and g is smaller by about 5%, when using polarizability data derived from optical data instead of theoretical values.

Another factor that impacts the value of the order parameter S is the orientation of the net dipole moment μ with respect to the main axis of inertia defined as angle β in the Maier−Meier formalism. However, the calculated angle β is derived for the charge-based molecular coordinates (so-called "standard orientation" in the Gaussian output file) rather than for mass-based coordinates required for the Maier−Meier theory. Fortunately molecular orientation in the two systems is similar and the error is not significant. Nevertheless, change of the angle β calculated for **2D** in 6-CHBT solutions (Table 3) to about half of the value (β = 3.4°) or doubling it (β = 15.0°) changes the order parameter S from 0.72 to 0.71 and 0.77, respectively.

The present implementation of the Maier−Meier theory contains some additional assumptions such as the density and reliance on a single conformer, that contribute to the overall error of the calculated parameters S and g. While the density affects the number density N and reaction field parameter F, conformational mobility impacts the dynamic anisotropy of polarizability $\Delta\alpha$ and angle β. Typically, however, molecular parameters α and μ are calculated for a single most elongated conformer with the assumption that it dominates in the condensed phase. This appears to be a reasonable assumption for rigid molecules such as **1** and **2**. Detailed computational analysis of 5CB demonstrated[13] that the most elongated conformer, which represents the global minimum on the potential energy surface, constitutes 40% of the mixture in the gas phase, and even higher populations of this conformer can be expected in the nematic phase. It was concluded that considering only the most stable conformer of 5CB gives negligible error to polarizability and dipole moment of less than 2%, when compared to an weighted average of parameters for four lowest energy conformers.[13] For more flexible molecules, however, consideration of two or more major conformers may be required for a more accurate representation of the molecule.[20] For instance, in an analysis of dielectric data for fluxional derivatives,[30] which quickly interconvert between two isomers *trans* and *cis*, and for extracting information about conformation population[32] weighted values of $\Delta\alpha$, μ, and β were used.

Most of assumptions of the Maier−Meier formalism and systematic shortcomings and errors of experimental methods and theoretical models are included in the calculated phase parameters g and S_{app}. Consequently, results obtained with the Maier−Meier formalism as described here are best used for comparative analysis within the same class of compounds in which molecular dipole moments and electronic polarizabilities, the main contributors to $\Delta\varepsilon$, are treated in the same way. Considering these and other limitations and assumptions in the Maier−Meier protocol, it is not clear whether extending the original Maier−Meier theory by including anisotropic solvent cavity with[72] or without atomistic details[73] will result in significant improvement in the accuracy of the method. Earlier studies concluded that contribution of shape anisotropy to the local field in anisotropic fluids can be neglected.[74]

Typically dielectric and optical parameters for additives are extrapolated from 10% w/w solutions in nematic hosts, and such parameters are host specific. For example, compounds **1D** and **2D** have $\Delta\varepsilon$ values of 3.8 and 11.3, respectively, obtained from a single point extrapolation in nematic host (FB-01),[23] while reported here $\Delta\varepsilon$ values obtained from 6-CHBT solutions are 8.6 and 13.6, respectively. These differences reflect additive-nematic solvent interactions, which can be analyzed as the g factor (aggregation, dielectric screening) and S_{app} (impact on material's order parameter), using the presented method. Both g and S_{app} can be considered as activity parameters for additives at low concentration solutions in nematic hosts. One of the assumptions of the presented method is that the additive has no effect on field and cavity factors F and h.[75] This might be correct for low concentration of relatively weakly polar additives (such as **1**), but for higher concentrations and strongly polar additives, their effect on factors F and h must be considered.

CONCLUSION AND SUMMARY

The Maier−Meier analysis of the extrapolated experimental dielectric data offers a valuable insight into behavior of additives in nematic mixtures, which is important for mixture formulation for LCD applications. Results for series **1** and **2** in 6-CHBT demonstrated that the anisometry of the molecular rigid core (size of the variable ring and the number of lateral fluorine atoms) impacts the order parameters S, and the Kirkwood factor g reflects the magnitude of the molecular dipole moment and the extent of association in solutions. Thus, trends apparent from the results demonstrate high S_{app} and low g for the carbocycles (**C** and **D**) and low S_{app} and high g for the carboranes (**A** and **B**).

The presented analysis relies on experimental data for the host (dielectric data, refractive index, and density), experimental dielectric data for solutions, and calculated dipole moment components and polarizability tensors of the additive. The resulting parameters S_{app} and g characterize the interaction

dx.doi.org/10.1021/jp411343a | J. Phys. Chem. B 2014, 118, 2238−2248

of the additive with the host (steric interactions, dielectric screening and associations) and permit a better understanding of the impact of the additive on material's properties.

Electronic parameters were obtained for a single conformer of the additive in the most elongated form using DFT methods, which appears to be sufficient for relatively rigid molecules. Analysis of computational results demonstrated that electronic polarizabilities calculated in dielectric medium of the solvent are closest to those observed experimentally. However, the polarizability anisotropy values $\Delta\alpha$ are significantly larger than the experimental values. Excessively large values of molecular dipole moments in the PCM calculations are corrected by the Kirkwood factor g in the Maier–Meier analysis.

Overall, despite numerous simplifications and assumptions in the Maier–Meier model and computational methods, the results provide good insight into behavior of polar additives in nematic solutions. The presented refined protocol for Maier–Meier analysis is particularly useful for comparative analysis of structurally similar additives in the same host, or an additive in several hosts.

■ ASSOCIATED CONTENT

Supporting Information

Synthetic details and analytical data for derivatives **1** and **2**, complete dielectric data, quantum-mechanical and Maier–Meier computational details, and archives for DFT geometry optimization. This material is available free of charge via the Internet at http://pubs.acs.org.

■ AUTHOR INFORMATION

Corresponding Author

*E-mail: (P.K.) Piotr.kaszynski@vanderbilt.edu.

Present Address

‡Institute of Chemistry, Military University of Technology, ul. Kaliskiego 2, 00–908 Warsaw, Poland.

Notes

The authors declare no competing financial interest.

■ ACKNOWLEDGMENTS

This project was supported by NSF Grants (DMR-0606317 and DMR-1207585). We are grateful to Prof. Stanisław Urban of Jagielonian University for helpful discussions and Dr. Eike Poetsch of E. Merck for the gift of boronic acid **4a**. This material is available free of charge via the Internet at http://pubs.acs.org.

■ REFERENCES

(1) Hird, M. Fluorinated Liquid Crystals – Properties and Applications. *Chem. Soc. Rev.* **2007**, *36*, 2070–2095.

(2) Reiffenrath, V.; Krause, J.; Plach, H. J.; Weber, G. New Liquid-Crystalline Compounds with Negative Dielectric Anisotropy. *Liq. Cryst.* **1989**, *5*, 159–170.

(3) Gray, G. W.; Hird, M.; Lacey, D.; Toyne, K. J. The Synthesis and Transition Temperatures of some 4,4″-Dialkyl- and 4,4″-Alkoxyalkyl-1,1′:4′,1″-terphenyls with 2,3- or 2′,3′-Difluoro Substituents and of Their Biphenyl Analogues. *J. Chem. Soc. Perkin Trans. 2* **1989**, 2041–2053.

(4) Demus, D.; Goto, Y.; Sawada, S.; Nakagawa, E.; Saito, H.; Tarao, R. Trifluorinated Liquid Crystals for TFT Displays. *Mol. Cryst. Liq. Cryst.* **1995**, *260*, 1–21.

(5) Kirsch, P.; Reiffenrath, V.; Bremer, M. Nematic Liquid Crystals with Negative Dielectric Anisotropy: Molecular Design and Synthesis. *Synlett* **1999**, 389–396.

(6) Klasen, M.; Bremer, M.; Tarumi, K. New Liquid-Crystal Materials for Active Matrix Displays with Negative Dielectric Anisotropy and Low Rotational Viscosity. *Jpn. J. Appl. Phys.* **2000**, *39*, L1180–L1182.

(7) Sun, G.-X.; Chen, B.; Tang, H.; Xu, S.-Y. Synthesis and Physical Properties of Novel Liquid Crystals Containing 2,3-Difluorophenyl and 1,3-Dioxane Units. *J. Mater. Chem.* **2003**, *13*, 742–748.

(8) Huh, I.-K.; Kim, Y.-B. New Low Viscosity Liquid Crystal Compounds Containing the 2,3,4-Trifluorophenyl Moiety for Active Matrix displays. *Liq. Cryst.* **2002**, *29*, 1265–1273.

(9) Bremer, M.; Lietzau, L. 1,1,6,7-Tetrafluoroindanes: Improved Liquid Crystals for LCD-TV Application. *New J. Chem.* **2005**, *29*, 72–74.

(10) Luo, F. C. In *Liquid Crystals: Applications and Uses*; Bahadur, B.; World Scientific: Singapore, 1990; Vol. *1*, pp 397–436 and references therein.

(11) Kirsch, P.; Bremer, M. Nematic Liquid Crystals for Active Matrix Displays: Molecular Design and Synthesis. *Angew. Chem., Int. Ed.* **2000**, *39*, 4216–4235.

(12) Pauluth, D.; Tarumi, K. Advanced Liquid Crystals for Television. *J. Mater. Chem.* **2004**, *14*, 1219–1227.

(13) Demus, D.; Inukai, T. Calculation of Molecular, Dielectric and Optical Properties of 4-*n*-Pentyl-4-cyano-biphenyl (5CB). *Liq. Cryst.* **1999**, *26*, 1257–1266.

(14) Urban, S.; Kędzierski, J.; Dąbrowski, R. Analysis of the Dielectric Anisotropy of Typical Nematics with the Aid of the Maier-Meier Equations. *Z. Naturforsch.* **2000**, *55A*, 449–456.

(15) Jadżyn, J.; Czerkas, S.; Czechowski, G.; Burczyk, A.; Dąbrowski, R. On the Molecular Interpretation of the Static Dielectric Properties of Nematic Liquid Crystals. *Liq. Cryst.* **1999**, *26*, 437–442.

(16) Dąbrowski, R.; Jadżyn, J.; Dziaduszek, J.; Stolarz, Z.; Czechowski, G.; Kasprzyk, M. The Physical and Molecular Properties of New Low Melting nematics with Negative Dielectric Anisotropy. *Z. Naturforsch.* **1999**, *54a*, 448–452.

(17) Jadżyn, J.; Czechowski, G.; Bauman, D. Static and Dynamic Dielectric Polarization and Viscosity of n-Hexylcyanobiphenyl in the Isotropic and Nematic Phases. *Z. Naturforsch.* **2000**, *55a*, 810–816.

(18) Huh, I.-K.; Kim, Y.-B. Numerical Evaluation of the Temperature Dependence of $\Delta\epsilon/S$ in 2,3,4-trifluorophenyl Liquid Crystals. *Jpn. J. Appl. Phys.* **2003**, *42*, 570–571.

(19) Xu, J.; Okada, H.; Sugimori, S.; Onnagawa, H. Numerical Evaluation of the Relative Value of Dielectric Anisotropy and Order Parameter in Fluorinated Nematic Liquid Crystals. *Jpn. J. Appl. Phys.* **2001**, *40*, 1375–1376.

(20) Bremer, M.; Tarumi, K. Gas Phase Molecular Modeling of Liquid Crystals: Electro-optical Anisotropies. *Adv. Mater.* **1993**, *5*, 842–848.

(21) Klasen, M.; Bremer, M.; Götz, A.; Manabe, A.; Naemura, S.; Tarumi, K. Calculation of Optical and Dielectric Anisotropy of Nematic Liquid Crystals. *Jpn. J. Appl. Phys.* **1998**, *37*, L945–L948.

(22) Saitoh, G.; Satoh, M.; Hasegawa, E. Estimating Dielectric Anisotropy of Liquid Crystal Compounds. *Mol. Cryst. Liq. Cryst.* **1997**, *301*, 13–18.

(23) Naemura, S. In *Physical Properties of Liquid Crystals: Nematics*; Dunmur, D., Fukuda, A., Luckhurst, G., Eds; IEE: London, 2001; pp 523–581.

(24) Maier, W.; Meier, G. A Simple Theory of the Dielectric Characteristics of Homogenous Oriented Liquid-Crystalline Phase of the Nematic Type. *Z. Naturforsch.* **1961**, *16A*, 262–267.

(25) Onsager, L. Electric Moments of Molecules in Liquids. *J. Am. Chem. Soc.* **1936**, *58*, 1486–1493.

(26) Dunmur, D.; Toriyama, K. In *Handbook of Liquid Crystals*; Demus, D., Goodby, J., Gray, G. W., Spiess, H.-W., Vill, V., Eds.; Wiley-VCH: Weinheim, Germany, **1998**; Vol *1*, pp 231–252.

(27) Urban, S. In *Physical Properties of Liquid Crystals: Nematics*; Dunmur, D. A., Fukuda, A., Luckhurst, G. R., Eds; IEE: London, 2001; pp 267–276.

(28) For details, see the Supporting Information.

(29) Januszko, A.; Glab, K. L.; Kaszynski, P.; Patel, K.; Lewis, R. A.; Mehl, G. H.; Wand, M. D. The Effect of Carborane, Bicyclo[2.2.2]-

octane and Benzene on Mesogenic and Dielectric Properties of Laterally Fluorinated Three-Ring Mesogens. *J. Mater. Chem.* **2006**, *16*, 3183−3192.
(30) Ringstrand, B.; Kaszynski, P. High Δε Nematic Liquid Crystals: Fluxional Zwitterions of the [*closo*-1-CB_9H_{10}]$^-$ Cluster. *J. Mater. Chem.* **2011**, *21*, 90−95.
(31) Ringstrand, B.; Kaszynski, P.; Januszko, A.; Young, V. G., Jr. Polar Derivatives of the [*closo*-1-CB_9H_{10}]$^-$ Cluster as Positive Δε Additives to Nematic Hosts. *J. Mater. Chem.* **2009**, *19*, 9204−9212.
(32) Nagamine, T.; Januszko, A.; Kaszynski, P.; Ohta, K.; Endo, Y. Mesogenic and Dielectric Properties of 5-Substituted 2-[12-(4-pentyloxyphenyl)-*p*-carboran-1-yl][1,3]dioxanes. *J. Mater. Chem.* **2006**, *16*, 3836−3843.
(33) Chen, Y.; Sun, J.; Xianyu, H.; Wu, S.-T.; Liang, X.; Tang, H. High Birefringence Fluoro-terphenyls for Thin-cell-gap TFT- LCDs. *J. Disp. Technol.* **2011**, *7*, 478−481.
(34) Yamamoto, H.; Takeshita, F.; Terashima, K.; Kubo, Y.; Goto, Y.; Sawada, S.; Yano, S. Liquid Crystalline Compounds Having 1,2,3-Trifluorophenyl Substituent for AM-LCDs TFTs with Low Voltage IC Driver. *Mol. Cryst. Liq. Cryst.* **1995**, *264*, 57−65.
(35) Dąbrowski, R. Isothiocyanates and their Mixtures with A Broad Range of Nematic Phase. *Mol. Cryst. Liq. Cryst.* **1990**, *191*, 17−27.
(36) Wu, S.-T.; Coates, D.; Bartmann, E. Physical Properties of Chlorinated Liquid Crystals. *Liq. Cryst.* **1991**, *10*, 635−646.
(37) Frisch, M. J.; Trucks, G. W.: Schlegel, H. B.; Scuseria, G. E.: Robb, M. A.; Cheeseman, J. R.; et al. *Gaussian 09*, Revision A.02, Gaussian, Inc.: Wallingford CT, 2009.
(38) Cossi, M.; Scalmani, G.; Rega, N.; Barone, V. New Developments in the Polarizable Continuum Model for Quantum Mechanical and Classical Calculations on Molecules in Solution. *J. Chem. Phys.* **2002**, *117*, 43−54.
(39) Alternative methods for preparation of **1D** and **2D** by the Suzuki coupling protocol were reported recently: Huang, M.; Cheng, J.; Tao, X.; Wei, M.; Shen, D. Application of Suzuki Cross-Coupling Reaction Catalyzed by Ligandless Palladium Chloride in the Synthesis of Liquid Crystals. *Synth. Commun.* **2007**, *37*, 2203−2208. Liu, N.; Liu, C.; Jin, Z. Green Synthesis of Fluorinated Biaryl Derivatives via Thermoregulated Ligand/palladium-catalyzed Suzuki Reaction. *J. Organomet. Chem.* **2011**, *696*, 2641−2648.
(40) Jasinski, M.; Jankowiak, A.; Januszko, A.; Bremer, M.; Pauluth, D.; Kaszynski, P. Evaluation of Carborane-containing Nematic Liquid Crystals for Electro-optical Applications. *Liq. Cryst.* **2008**, *35*, 343−350.
(41) Douglass, A. G.; Pakhomov, S.; Reeves, B.; Janoušek, Z.; Kaszynski, P. Triphenylsilyl as a Protecting Group in the Synthesis of 1,12-Heterodisubstituted i-Carboranes. *J. Org. Chem.* **2000**, *65*, 1434−1441.
(42) Janoušek, Z.; Kaszynski, P. Heterodisubstituted 1,10-dicarba-*closo*-Decaboranes from Substituted *nido*-Carborane Precursors. *Polyhedron* **1999**, *18*, 3517−3526.
(43) Ringstrand, B.; Vroman, J.; Jensen, D.; Januszko, A.; Kaszynski, P.; Dziaduszek, J.; Drzewinski, W. Three- and Four-ring Mesogenic Esters Containing p-Carborane, Bicyclo[2.2.2]octane, Cyclohexane, and Benzene. *Liq. Cryst.* **2005**, *32*, 1061−1070.
(44) Löbbert, A.; Kitney, S. P.; Kelly, S. M.; O'Neill, M.; Stirner, T. Terminal end-Group Efficiency for the Nematic Phase using Model Bicyclo[2.2.2]octanes. *Liq. Cryst.* **2007**, *34*, 1357−1367.
(45) Aziz, N.; Kelly, S. M.; Duffy, W.; Goulding, M. Rod-shaped Dopants for Flexoelectric Nematic Mixtures. *Liq. Cryst.* **2009**, *36*, 503−520.
(46) Eidenschink, R. Low Viscous Compounds of Highly Nematic Character. *Mol. Cryst. Liq. Cryst.* **1983**, *94*, 119−125.
(47) Müller, H. J.; Haase, W. Refractive Indices, Density and Order Parameters for some Biphenyl Cyclohexanes. *Mol. Cryst. Liq. Cryst.* **2004**, *409*, 127−135.
(48) Czuprynski, K.; Douglass, A. G.; Kaszynski, P.; Drzewinski, W. Carborane-Containing Liquid Crystals: A Comparison of 4-Octyloxy-4′-(12-pentyl-1,12-dicarbadodecaboran-1-yl)biphenyl with Its Hydrocarbon Analogs. *Liq. Cryst.* **1999**, *26*, 261−269.
(49) Czuprynski, K.; Kaszynski, P. Homostructural Two-ring Mesogens: A Comparison of *p*-Carboranes, Bicyclco[2.2.2]octane and Benzene as Structural Elements. *Liq. Cryst.* **1999**, *26*, 775−778.
(50) Januszko, A.; Kaszynski, P.; Drzewinski, W. Ring Effect on Helical Twisting Power of Optically Active Mesogenic Esters Derived from Benzene, Bicyclo[2.2.2]octane, and *p*-Carborane Carboxylic Acids. *J. Mater. Chem.* **2006**, *16*, 452−461.
(51) Ohta, K.; Januszko, A.; Kaszynski, P.; Nagamine, T.; Sasnouski, G.; Endo, Y. Structural Effects in Three-Ring Mesogenic Derivatives of *p*-Carborane and Their Hydrocarbon Analogs. *Liq. Cryst.* **2004**, *31*, 671−682.
(52) Kaszynski, P. In *Boron Science: New Technologies & Applications*; Hosmane, N., Ed.; CRC Press: 2012; p 305−338.
(53) The geometrical parameters for each ring were calculated (HF/6-31G(d)) and corrected for H and C (benzene) van der Waals radii (1.2 Å and 1.7 Å respectively). Benzene was treated as an ellipsoid, and the diameter d represents an average of the two axes *a* and *b*: **A**, d = 7.43 Å; **B**, *d* = 7.17 Å; **C**, *d* = 6.72 Å; **D**, *d* = 5.965 Å (*a* = 6.70 Å, *b* = 5.23 Å).
(54) Li, J.; Wu, S.-T. Self-consistency of Vuks Equations for Liquid-Crystal Refractive Indices. *J. Appl. Phys.* **2004**, *96*, 6253−6258.
(55) Vuks, M. F. Determination of Optical Anisotropy of Aromatic Molecules from Double Refreaction of Crystals. *Opt. Spectrosk.* **1966**, *20*, 361−364.
(56) Haller, I.; Huggins, H. A.; Lilienthal, H. R.; McGuire, T. R. Order-Related Properties of Some Nematic Liquids. *J. Phys. Chem.* **1973**, *77*, 950−954.
(57) Haldar, S.; Barman, S.; Mandal, P. K.; Haase, W.; Dabrowski, R. Influence of Molecular Core Structure and Chain Length on the Physical Properties of Nematogenic Fluorobenzene Derivatives. *Mol. Cryst. Liq. Cryst.* **2010**, *528*, 81−95.
(58) Douglass, A. G.; Czuprynski, K.; Mierzwa, M.; Kaszynski, P. An Assessment of Carborane-containing Liquid Crystals for Potential Device Application. *J. Mater. Chem.* **1998**, *8*, 2391−2398.
(59) Clark, S. In *Physical Properties of Liquid Crystals: Nematics*, Dunmur, D. A., Fukuda, A., Luckhurst, G. R., Eds; IEE: London, 2001; pp 113−123.
(60) Smith, J. W. *Electric Dipole Moments*; Butterworths: London, 1955.
(61) Prezhdo, V. V.; Degtereva, L. I.; Lutskii, A. E. Intermolecular Field Interaction in Solutions and the Effective Dipole Moment of Molecules. *J. Gen. Chem. USSR* **1981**, *51*, 772−777.
(62) The factor *g* relates μ^2 and μ_{eff}^2 Bordewijk, P. Extension of the Kirkwood-Fröhlich Theory of the Static Dielectric Permittivity to Anisotropic Liquids. *Physica* **1974**, *75*, 146−156.
(63) Hansch, C.; Leo, A.; Taft, R. W. A Survey of Hammett Substituent Constants and Resonance and Field Paramaters. *Chem. Rev.* **1991**, *91*, 165−195.
(64) Zakharkin, L. I.; Kalinin, V. N.; Rys, E. G. The Electronic Effects of 1-para-Carboranyl Group (p-$B_{10}H_{10}C_2H$-). *Bull. Acad. Sci. USSR, Div. Chem. Sci.* **1974**, 2543−2545.
(65) Zakharkin, L. I.; Kalinin, V. N.; Rys, E. G.; Kvasov, B. A. Electronic Effects of 1-[1,6-Dicarbaclosodecaborane(10)] and 1-[1,10-Dicarbaclosodecaborane(10)] Groups. *Bull. Acad. Sci. USSR, Div. Chem. Sci.* **1972**, 458−460.
(66) The σ_p value for adamantane was used instead: Alper, H.; Keung, E. C. H.; Partis, R. A. The Effects of Aliphatic and Cycloalkyl Substituents on a Ring-Chain Tautomeric Equilibrium. *J. Org. Chem.* **1971**, *36*, 1352−1355 footnote 31.
(67) Charton, M. Electrical Effect Substituent Constants for Correlation Analysis. *Prog. Phys. Org. Chem.* **1981**, *13*, 119−251.
(68) Kaszynski, P.; Pakhomov, S.; Tesh, K. F.; Young, V. G., Jr. Carborane-containing Liquid Crystals: Synthesis and Structural, Conformational, Thermal, and Spectroscopic Characterization of Diheptyl and Diheptynyl Derivatives of *p*-Carboranes. *Inorg. Chem.* **2001**, *40*, 6622−6631.
(69) Raszewski, Z.; Dąbrowski, R.; Stolarzowa, Z.; Żmija, J. Dielectric studies on binary mixtures containing 4-*trans*-4′-*n*-hexyl-cyclohexyl-isothiocyanato-benzene. *Cryst. Res. Technol.* **1987**, *22*, 835−844.

(70) Kędziora, P.; Jadżyn, J. Dimerization of Polar Mesogenic Molecules. *Mol. Cryst. Liq. Cryst.* **1990**, *192*, 31−37.
(71) Typically optical data is obtained at 589 nm, while theoretical values are usually calculated at static field. The difference in α is small and negligable, it can however be significant for $\Delta\alpha$.
(72) Ferrarini, A. Dielectric Permittivity of Nematics with a Molecular Based Continuum Model. *Mol. Cryst. Liq. Cryst.* **2003**, *395*, 233−252.
(73) Baran, J. W.; Kędzierski, J.; Raszewski, Z.; Żmija, J. The Relation Between Dielectric Permittivity of Liquid Crystals and Their Molecular Parameters. *Elect. Techn.* **1979**, *12*, 107−114.
(74) Dunmur, D. A.; Munn, R. W. The Shape of the Lorentz Cavity and the Internal Field in Anisotropic Fluids. *Chem. Phys.* **1983**, *76*, 249−253.
(75) More on calculation of parameters F and h in Zhang, R.; He, J.; Peng, Z.-H.; Li, X. Calculating the dielectric anisotropy of nematic liquid crystals: a reinvestigation of the Maier-Meier theory. *Chin. Phys. B.* **2009**, *18*, 2885−2892.